The AAPS Journal (2020) 22:67
DOI: 10.1208/s12248-020-00445-0

Research Article

Comparison of Alternative Population Modeling Approaches for Implementing a Level A IVIVC and for Assessing the Time-Scaling Factor Using Deconvolution and Convolution-Based Methods

Roberto Gomeni[1,2] and Françoise Bressolle-Gomeni[1]

Received 5 February 2020; accepted 6 March 2020

Abstract. Different approaches based on deconvolution and convolution analyses have been proposed to establish IVIVC. A new implementation of the convolution-based model was used to evaluate the time-scaled IVIVC using the convolution (method 1) and the deconvolution-based (method 2) approaches. With the deconvolution-based approach, time-scaling was detected and estimated using Levy's plots while with the convolution-based approach, time-scaling was directly determined by a time-scaling sub-model of the convolution integral model by nonlinear regression. The objectives of this study were (i) to show how time-scaled deconvolution and convolution-based approaches can be implemented using population modeling approach using standard nonlinear mixed-effect modeling software such as NONMEM and R, and (ii) to compare the performances of the two methods for assessing IVIVC using complex *in vivo* drug release process. The impact of different PK scenarios (linear and nonlinear PK disposition models, and increasing levels of inter-individual variability (IIV) on *in vivo* drug release process) was considered. The performances of the methods were assessed by computing the prediction error (%PE) on C_{max}, AUC, and partial AUC values. The mean %PE values estimated with the two methods were compliant with the IVIVC validation criteria. However, different from convolution-based, deconvolution-based approach showed that (i) the increase of IIV on *in vivo* drug release significantly affects the maximal %PE values of C_{max} leading to failure of IVIVC validation, and (ii) larger %PE values for C_{max} were associated to complex nonlinear PK disposition models. These results suggest that convolution-based approach could be considered at preferred approach for assessing time-scaled IVIVC.

KEY WORDS: convolution-based IVIVC; deconvolution-based IVIVC; NONMEM; population approach; time-scaling.

INTRODUCTION

A critical step in the development and in the optimization of dosage forms is the assessment of the relationship between *in vitro* drug release and time course of the *in vivo* drug concentrations (IVIVC).

The IVIVC is a tool not only for reducing the number of comparative bioavailability studies but also for improving and optimizing the drug performances (1).

The most useful correlation is level A IVIVC where a point to point correlation between *in vitro* dissolution and *in vivo* absorption is established. Different approaches have been proposed to establish this correlation. These methods are generally classified as methods based on deconvolution and methods based on convolution analysis.

Among the deconvolution-based approaches, the methods of Wagner-Nelson and Loo-Riegelman were initially developed (2,3). These methods have been extensively used to determine the absorption kinetics following an oral administration with the assumption that the drug disposition was linear and described by a one- or by a two-compartment model. Numerical deconvolution methods were subsequently developed as alternative methods for calculating the drug input rates for generic PK models (4,5).

A number of concerns on the performances of these methodologies have been raised. These concerns were primarily associated with the assumptions and the approximations required by the numerical methods used to implement the deconvolution analysis (6). To overcome these limitations, convolution-based methods gained increasing

Electronic supplementary material The online version of this article (https://doi.org/10.1208/s12248-020-00445-0) contains supplementary material, which is available to authorized users.

[1] R&D, Pharmacometrica, Lieu-dit Longcol, 12270, La Fouillade, France.
[2] To whom correspondence should be addressed. (e–mail: roberto.gomeni@pharmacometrica.com)

Published online: 15 April 2020

interest for the assessment of IVIVC as these methods presented some appealing features with respect to the deconvolution-based methods such as their ability to conduct IVIVC using nonlinear mixed-effect modeling approach in one single analysis step (7,8).

The performances of the deconvolution and convolution-based approaches were compared in a study conducted on simulated data (9). In that study, the deconvolution analysis was performed using a dedicated software implementing a regularization method constrained to nonnegative values. This comparison showed that the convolution-based modeling approach accurately predicted the observed plasma concentration–time course, while the accuracy of the plasma concentration predicted using the deconvolution method failed to comply with the expected requirements of the FDA (6).

More recently, a new implementation of the convolution-based model has been proposed (1). One of the appealing features of this new implementation is the ability of the model not only to account for any parametric and nonparametric dissolution time course and any *in vivo* input function but also to estimate the time-scaling necessary to normalize the *in vitro* dissolution time scale in order to match that of the *in vivo* dissolution/absorption (10).

The assessment of IVIVC requires that the *in vitro* dissolution and *in vivo* input curves may be directly superimposable or may be made superimposable by the use of appropriate scaling factors when the timing of the dissolution and the *in vivo* release processes significantly differ (11). When used, time-scaling factors are requested to be the same for all formulations.

With the deconvolution-based approach, time-scaling is traditionally detected and estimated using Levy's plots where the time required to achieve a certain percent of the dose released/absorbed *in vivo* (obtained through deconvolution) is plotted against the time required to achieve the same percent of the dose released *in vitro*. A unitary slope with a zero-intercept line in the Levy's plot indicates similar time frame of the *in vitro* and *in vivo* processes; otherwise, a curvilinear shape of this plot indicates the presence of a different time frame for the two processes.

With the convolution-based approach, the time-scaling accounting for potential time differences in the *in vitro* and *in vivo* processes can be directly determined by estimating the parameters of a general time-scaling sub-model of the convolution integral model when estimating the IVIVC using a nonlinear regression (1).

The availability of these new computational tools raises a number of questions when the population approach is used to assess the time-scaled IVIVC. In particular what is the impact on the performance of deconvolution-based and convolution-based methods when (i) the PK disposition is described by linear or nonlinear processes, and (ii) the *in vivo* drug release is characterized by high inter-individual variability (IIV)?

The primary objective of this study was to show how the convolution-based (method 1) and the deconvolution-based (method 2) approaches, including the assessment of time-scaling and the Levy's plot generation, can be easily implemented using a standard nonlinear mixed-effect modeling software such as NONMEM and R without the need of dedicated software for numerical deconvolution.

The secondary objective was to compare the performances of the two methods for assessing IVIVC using (i): linear and nonlinear PK deposition models, and (ii) increasing levels of IIV in the *in vivo* drug release process. Clinical trial simulation was used to generate the time course of the drug dissolved over time and the time course of the plasma concentrations resulting from the administration of three extended release (ER) and one immediate release (IR) formulation to 12 subjects in a crossover study design. The data were simulated assuming the presence of a time-scaling between *in vitro* dissolution and *in vivo* absorption. The performances of the methods were assessed by estimating the prediction error on the individual C_{max}, AUC, and partial AUC (pAUC) values estimated using a population modeling approach.

METHODS

The Convolution-Based Model

The time course of the drug concentration (C_p) resulting from an arbitrary dose was described by a convolution model as a function of the *in vivo* drug release (f) and the disposition and elimination processes defined by the unit impulse response (UIR) function according to the convolution integral:

$$Cp(t) = \int_0^t f(\tau) \cdot \mathrm{UIR}(t-\tau) \cdot d\tau = f * \mathrm{UIR} \quad (1)$$

where f is the rate at which drug is released from a dosage form, and * is the symbol defining the convolution.

The function characterizing the drug delivery f was estimated as the first derivative of the cumulative drug release function r:

$$f(t) = \frac{\mathrm{dr}(t)}{\mathrm{dt}} \quad (2)$$

The convolution integral (Eq. 1) was represented in a more manageable form as system of differential equations (7). In case of a simple disposition process (say one compartment process (model 1)), the UIR function was characterized by the volume of distribution (V) and the first order elimination rate constant (k_{el}). In this scenario, the convolution integral was written as:

$$\frac{\mathrm{dAp}(t)}{\mathrm{dt}} = \mathrm{BI} \cdot \mathrm{Dose} \cdot \frac{\mathrm{dr}(t)}{\mathrm{dt}} - \mathrm{kel} \cdot \mathrm{Ap} \quad (3)$$

where Ap(t) is the amount of drug, and BI is the relative bioavailability of the current formulation with respect to the reference formulation (the one that provided an estimate of the UIR function).

To assess the potential implication of more complex models on the performances of the convolution and deconvolution-based time-scaled IVIVC, a nonlinear model UIR model (model 2) was considered:

$$\frac{dAp(t)}{dt} = BI \cdot Dose \cdot \frac{dr(t)}{dt} - Cp \cdot \frac{Vm}{Km + Cp} - k12 \cdot Ap + k21 \cdot A2 \quad (4)$$

$$\frac{dA2(t)}{dt} = k12 \cdot Ap - k21 \cdot A2$$

where Vm is the maximum elimination rate, and Km is the Michaelis-Menten constant (drug concentration at which the rate of elimination is 50% of Vm).

C_p was estimated as Ap(t)/V by numerical integration of Eqs. 3 and 4. These models can be easily generalizable to account for more complex and nonlinear disposition processes using the compartmental theory (12).

The r(t) function characterizes the dissolution/absorption process. In the context of the present analysis the same double Weibull model was used for the two UIR models:

$$r(t) = 1 - \left(FF \cdot e^{-\left(\left(\frac{t}{TD}\right)^{SS}\right)} + (1 - FF) \cdot e^{-\left(\left(\frac{t}{TD1}\right)^{SS1}\right)} \right) \quad (5)$$

where t is time, FF is the fraction of the dose released in the 1st process, TD and TD1 are times to release 63.2% of the dose in the 1st and in the 2nd process, and SS and SS1 are the sigmoidicity factors for the 1st and the 2nd process.

The solution of the differential equation models (Eqs. 3 and 4) required the estimate of the first derivative of the r(t), dr/dt. This was estimated using a finite difference approach:

$$\frac{dr}{dt} \cong \frac{r(t) - r(t + \Delta)}{\Delta} \quad (6)$$

where Δ is a sufficiently small number.

One of the benefits of representing the drug concentration (C_p) using a convolution-based model was the ability to easily conduct both convolution and deconvolution analyses using the same modeling framework.

The deconvolution analysis was conducted by fitting the convolution-based model to the observed data with the parameters defining the UIR function fixed to the values estimated in the analysis of the IR data. In this scenario, the only parameters estimated in the nonlinear regression were the parameters defining the r(t) function characterizing the *in vivo* drug release.

The convolution analysis was conducted by simulating the C_p values when the parameters defining the UIR function were fixed to the values estimated by fitting the IR data, and the parameters of the r(t) function were fixed to some reference value (for example, to the values estimated in the analysis of the *in vitro* dissolution data).

Data

Clinical trial simulation was used to generate the dissolution data of the three ER formulations with different release rates (form A, fast; form B, medium; and form C, slow), and the PK data of 12 subjects included in a crossover study where the same ER formulations and one IR formulation were administered.

The individual data were simulated using dissolution and *in vivo* PK data mimicking the dissolution and the PK time course of an ER formulation developed using the osmotic controlled-release oral-delivery-system OROS® of methylphenidate (MPH) (10). The *in vitro* dissolution data were simulated for each formulation at 0, 0.25, 0.5, 1, 1.5, 2, 2.5, 3, 3.5, 4, 5, 6, 8, 10, 12, 14, 17, 20, and 24 h. The *in vivo* PK data of the three ER and one IR formulation were simulated at 0, 0.25, 0.5, 0.75, 1, 1.25, 1.5, 1.75, 2, 2.5, 3, 3.5, 4, 4.5, 5, 6, 7, 7.5, 8, 9, 10, 11, 12, 13, 14, 15, 16, 18, 20, 22, and 24 h post dose. *Simulation of the Dissolution Data.* The dissolution data of the three formulations were described by the double Weibull model (Eq. 5). The parameters of the model were selected to assure a sufficiently distinct time course of drug release using the following assumptions: (i) 20% of the dose was released in the first dissolution process for the three formulations (FF = 0.2), (ii) the time necessary to dissolve 50% of the dose was ~ 35% faster for the formulation A that for the reference formulation B, and (iii) the time necessary to dissolve 50% of the dose was ~ 35% slower for the formulation C than for the reference formulation B. The dissolution measurements were simulated assuming a residual error normally distributed with a variance of 0.5 ($\%^2$).

Simulation of the IR Data. The individual IR PK data were generated assuming two different UIR models: a one-compartment model (Eq. 7)

$$\frac{dAb(t)}{dt} = -ka \cdot Ab$$
$$\frac{dAc(t)}{dt} = ka \cdot Ab - kel \cdot Ac \quad (7)$$

and a two-compartment model with nonlinear elimination (Eq. 8).

$$\frac{dAb(t)}{dt} = -ka \cdot Ab$$
$$\frac{dAc(t)}{dt} = ka \cdot Ab - Cp \cdot \frac{Vm}{Km + Cp} - k12 \cdot Ap + k21 \cdot A2 \quad (8)$$
$$\frac{dAp(t)}{dt} = k12 \cdot Ap - k21 \cdot A2$$

where ka and kel are the first order absorption and elimination constants, V the volume of distribution, Vm is the maximum elimination rate, Km is the Michaelis-Menten constant, and k12 and k21 are the first order transfer rate constants from/to the central and the peripheral compartment. Ab, Ac, and Ap are the amount of drug at the absorption site, in the central compartment, and in the peripheral compartment, respectively. C_p is the drug concentration estimated as Ac(t)/V. For the two models, the inter-individual variability was assumed log-normally distributed and the residual error model was assumed to be a combined additive and proportional model.

The following population parameters were used in the simulations:

- Model 1, ka = 2.02 (hr^{-1}), k_{el} = 0.25 (hr^{-1}), V = 2.94 (L). Each parameter was assumed log-normally distributed with an inter-individual variability (IIV) defined by a coefficient of variation of 30%. The additive and proportional residual errors were characterized by a variance of 0.08 and 0.0634, respectively. These parameter values were selected to mimic the population PK parameters of MPH IR formulation (1).
- Model 2, ka = 1.25 (hr^{-1}), k12 = 0.02 (hr^{-1}), k21 = 0.385 (hr^{-1}), Vm = 5.2 (ng/h), Km = 10 (ng/mL), V = 0.484 (L). Each parameter was assumed log-normally distributed with an inter-individual variability (IIV) defined by a coefficient of variation of 20%. The additive and proportional residual errors were characterized by a variance of 0.0112 and 0.0243, respectively.

The IIV and the residual error parameters for model 2 were fixed at lower values than the ones of model 1 to avoid parameter identifiability issues due to the limited sample size and the nonlinearity of the model.

Simulation of the ER Data. The simulation of the individual concentrations of the three formulations in the 12 subjects was conducted in three steps:

1. Fit the data describing the three individual dissolution profiles generated in the simulation step of the dissolution data using Eq. 5;
2. Fit the IR data using a population PK approach and estimate the individual disposition and elimination PK parameters of model 1 and 2;
3. Simulate the individual ER PK concentrations for the three formulations in the 12 subjects using Eqs. 3 and 4 where the individual UIR parameters (V_i, kel_i and V_i, $k12_i$, $k21_i$, Vm_i, and Km_i) were fixed to the values estimated in step 2. The BI parameter was fixed to 1, and the parameters of Eq. 5 of the three formulations were fixed to the values estimated in step 1. The five parameters of the Weibull function (TD, SS, TD1, SS1, and FF) were assumed to be log-normally distributed to account for the *in vivo* IIV in the drug release. The impact of four levels of IIV (20%, 30%, 40%, 50%) on the performance of the convolution-based and deconvolution-based approaches were evaluated.

A time-scaling function was included in the simulation model to account for time differences in the *in vitro* and the *in vivo* processes:

$$\begin{aligned} r_{vivo}(t) &= r_{vitro}(tt) \\ tt &= b_2 \cdot t^{b_3} \end{aligned} \tag{9}$$

where r_{vitro} is the function associated with the dissolution of the three formulations estimated in step 1 and r_{vivo} is the drug delivery function used in the simulation of the ER profiles. In case of absence of time-scaling between r_{vivo} and r_{vitro}, $b_2 = 1$ and $b_3 = 1$.

Implementing IVIVC

Two methods were used in the IVIVC analysis that was conducted in four steps using the convolution-based (method 1) and the deconvolution (method 2) approaches as schematically presented in Fig. 1. Step 1, 2, and 4 were common to the two methods while step 3 was specific for each of the two methods.

Step 1 included the modeling of the dissolution data, step 2 included the population PK analysis of the UIR function using IR data, and step 4 included the model validation procedures conducted by comparing the observed and model predicted *in vivo* data.

Step 3: *Method 1.* This was a one-step analysis based on the population fitting of the convolution-based model (Eqs. 3 and 4) to the ER data. In this model, the individual parameters defining the UIR function were fixed to the values estimated in step 2, and the parameters of the r(t) function were fixed to the values estimated in the analysis of the dissolution data (step 1). The only parameters estimated in the nonlinear regression were the parameters of the time-scaling sub-model (Eq. 9) (1):

$$\begin{aligned} r_{vivo}(t) &= a_1 + a_2 \cdot r_{vitro}(tt) \\ tt &= b_1 + b_2 \cdot t^{b_3} \end{aligned} \tag{10}$$

This general time-scaling function can account for different linear and nonlinear behavior according to the estimated values of the parameters a_1, a_2, b_1, b_2, and b_3. In case of absence of time-scaling, $a_1 = 0$, $a_2 = 1$, $b_1 = 0$, $b_2 = 1$, and $b_3 = 1$.

The performance of alternative time-scaling nested models was evaluated using the objective function value (OFV) representing minus twice the log of the likelihood estimated by NONMEM and the likelihood ratio test. This test was based on the change of OFV ($\Delta OFV = [OFV_{full} - OFV_{reduced}]$) associated with a full and a reduced model. The ΔOFV was chi-squared (χ^2) distributed with degree of freedom equal to the difference of the number of parameters in the two models. An example of model's comparison is when a full model is evaluated against a reduced model (with a difference of 3 parameters). A change in OFV ≥ 7.81 is required for the full model to be statistically better than the reduced model ($p < 0.05$, df = 3); otherwise, the reduced model was considered the preferred one (13).

Method 2. This analysis was conducted in four stages:

1. Deconvolution analysis by nonlinear regression to estimate the individual *in vivo* input functions (parameters of Eq. 5) using the convolution-based model (Eqs. 3 and 4) with the UIR parameters fixed to the individual PK parameters (V_i,kel_i and V_i, $k12_i$, $k21_i$, Vm_i, and Km_i) estimated in step 2.
2. Generation of the Levy's plot by estimating the time required to release *in vitro* and to absorb *in vivo* the same percentage of the dose using the outcomes of stage 1. This analysis was conducted using an *R* script.

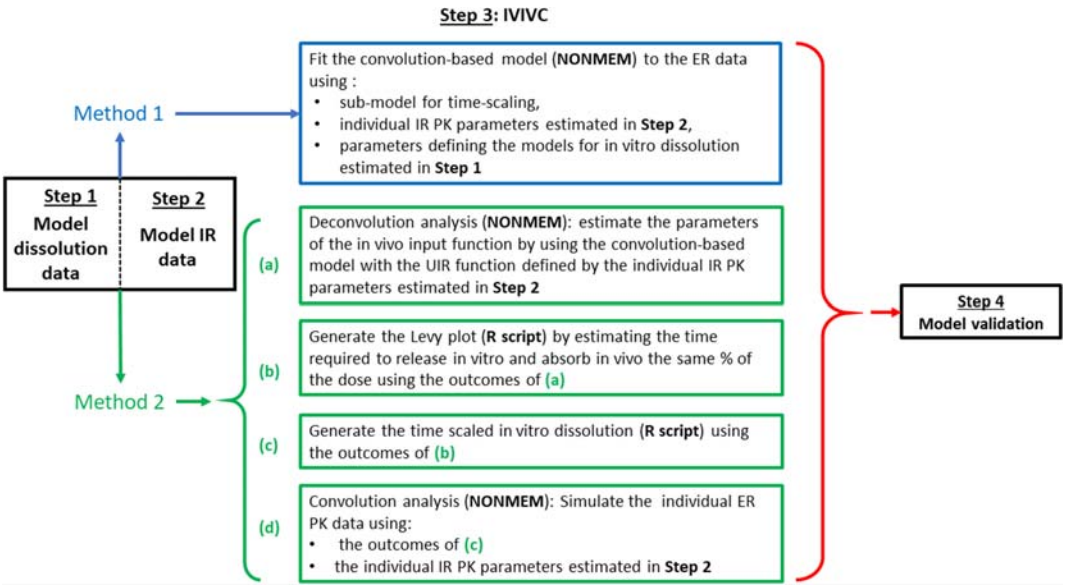

Fig. 1. Schematic representation of the IVIVC analyses conducted with the convolution-based (method 1) and the deconvolution-based (method 2) approaches

3. Generation of the time-scaled *in vitro* dissolution using the outcomes of stage 2. This analysis was conducted using an *R* script.
4. Convolution analysis to simulate the individual ER drug concentrations using the outcomes of stage 3, and the individual PK parameters (V_i, kel_i and V_i, $k12_i$, $k21_i$, Vm_i, and Km_i) estimated in step 2.

The Levy's plot was used to evaluate the relationship between *in vitro* and *in vivo* time frame of the three formulations. The plot was generated by graphically displaying the time needed for *in vivo* absorption *versus* the time needed for *in vitro* dissolution of a particular amount of drug from the dosage form (i.e., 0.1, 0.2, 0.3, 0.4, 0.5, 0.6, 0.7, 0.8, 0.9, 1%).

The deviation from the identity line of the generated curve indicates that the time frame of the *in vitro* and the *in vivo* processes was not the same requiring the use of a time-scaling factor for estimating the *in vitro* times of percentage dissolved equivalent to percentage absorbed. According to the current FDA guidelines, the introduction of a time scale factor is acceptable as long as it is used for all formulations and for all further applications of the IVIVC model.

The Levy's plot was generated using the parameters resulting from the fitting of the dissolution data and from the deconvolution analysis conducted on the individual plasma concentrations. The Levy's plot required the estimate of the time when the same amount of drug was dissolved or released from the dosage form. At this purpose, the R code implementing this analysis interpolated the *in vitro* and the *in vivo* data using the "optimize" function to compute the exact times when the same amount of drug was dissolved or released from the dosage form (14).

The LOESS smoothing function was used to characterize the relationship between the time (t) necessary to absorb a given fraction of the dose (Abs_t) and that necessary to dissolve the same fraction of the dose (Dis_t). LOESS short for locally weighted scatter-plot smoother is a nonparametric approach for fitting a smooth curve between an independent and a dependent variable (15). Two LOESS functions were derived: the first one (afd) estimated the time (t) necessary to absorb a given fraction of the dose (Abs_t) as a function of the time necessary to dissolve the same fraction of the dose (Dis_t): $Abs_t = afd\ (Dis_t)$, and the second one (dfa) estimated the time (t) necessary to dissolve a given fraction of the dose as a function of the time necessary to absorb the same fraction of the dose (Abs_t) $Dis_t = dfa\ (Abs_t)$.

The only requirement of this methodology was that the relationship between dependent and independent variables can be locally approximated with a member of a simple class of parametric function.

The time-scaled dissolution data ($DisScal_{PKt}$) at the time

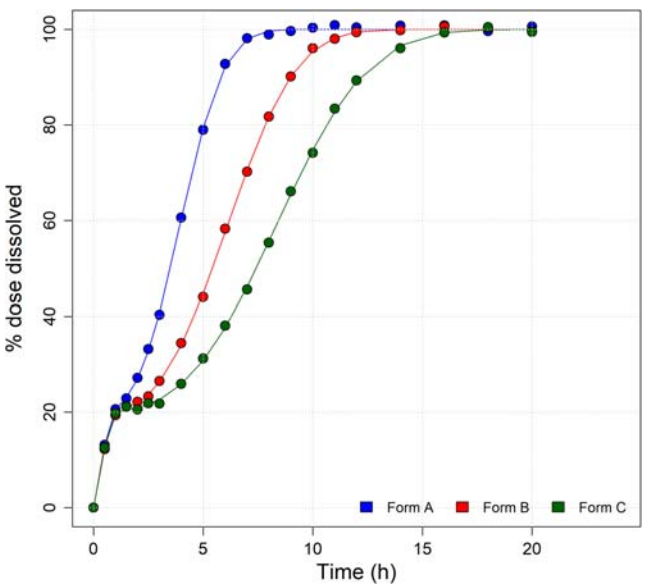

Fig. 2. Simulated (dots) and model predicted (solid lines) dissolution data for the three formulations

Table I. Convolution-Based Approach: Estimated Time-Scaling Parameter Values in the IVIVC Analysis for Model 1 and Model 2

	Run 1		Run 2			Run 1		Run 2	
Parameter	Estimate	RSE	Estimate	RSE	Parameter	Estimate	RSE	Estimate	RSE
Model 1: IIV = 0%					Model 2: IIV = 0%				
*a*1	0	#	0*		*a*1	− 0.01	20.40%	0*	
*a*2	1	4.70%	1*		*a*2	1.01	0.10%	1*	
*b*1	0.01	#	0*		*b*1	0.01	24.00%	0*	
*b*2	0.22	#	0.23	5.40%	*b*2	0.21	4.40%	0.22	4.40%
*b*3	1.57	#	1.55	2.20%	*b*3	1.61	1.00%	1.58	1.50%
OFV	878.101		880.232		OFV	5370.134		4312.349	
ΔOFV			2.131		ΔOFV			− 1057.79	
Model 1: IIV = 20%					Model 2: IIV = 20%				
*a*1	0	32.60%	0*		*a*1	0	11.20%	0*	
*a*2	1	0.10%	1*		*a*2	1	0.00%	1*	
*b*1	0	88.30%	0*		*b*1	0	32.60%	0*	
*b*2	0.2	1.80%	0.2	3.90%	*b*2	0.2	86.50%	0.2	2.80%
*b*3	1.61	1%	1.6	1.40%	*b*3	1.61	14.30%	1.6	0.80%
OFV	−2358.805		−2355.78		OFV	853.794		858.633	
ΔOFV			3.021		ΔOFV			4.839	
	IIV (CV%)		IIV (CV%)			IIV (CV%)		IIV (CV%)	
TD (hour)	18.03%		18.22%		TD (hour)	17.52%		17.80%	
SS (unitless)	17.18%		17.09%		SS (unitless)	17.32%		17.55%	
TD1(hour)	19.65%		19.60%		TD1(hour)	19.52%		19.62%	
SS1(unitless)	17.86%		17.80%		SS1(unitless)	18.89%		17.86%	
FF (%)	20.15%		20.10%		FF (%)	19.72%		20.10%	

of the PK measurements (PKt) were estimated using the following relationship: $\text{DisScal}_{\text{PKt}} = r\ [\text{dfa (PKt)}]$; where r is the model defining the double Weibull equation (Eq. 5). The approximated first derivative of the time-scaled dissolution data was computed as:

$$\frac{\text{dDisScalPKt}}{\text{dt}} \cong \frac{\text{DisScal(PKt)} - \text{DisScal(PKt} + \Delta)}{\Delta} \tag{11}$$

where Δ is a sufficiently small number.

The first derivative of the time-scaled dissolution data was required to estimate the *in vivo* PK time course using the convolution analysis (Eqs. 3 and 4).

IVIVC Model Validation

Model validation was the final step in the IVIVC analysis. This step of the analysis was aimed to provide quantified evidence of the predictive performance of the model using data from the formulations used to build the model (internal validation) or using data obtained from a different (new) formulation (external validation). The internal validation was implemented using the IVIVC models developed for each formulation by comparing the model predicted to the expected PK values in each simulation scenario considered. The prediction error (%PE) was computed for each PK parameter using the equation:

$$\%\text{PE} = \frac{1}{n}\sum_{1}^{n}\frac{|\text{Observed value} - \text{Predicted value}|}{\text{Observed value}} \cdot 100 \tag{12}$$

where n is the number of formulations.

The criterion for assessing the level of predictability was for each PK parameter, the average %PE ≤ 10% with no individual values > 15%. If this criterion was not met, the evaluation of external predictability was required (11).

In addition to $\text{AUC}_{0\text{-inf}}$ and $C_{\max}$, specific metrics based on the concept of partial AUC (pAUC) were recently recommended by the FDA for extended release formulations of drugs with complex PK time course such as the one considered in the present analysis (16). Therefore, the following pAUC parameters were also evaluated:

- $\text{pAUC}_{0\text{–}3}$, AUC from 0 to 3 h,
- $\text{pAUC}_{3\text{–}7}$, AUC from 3 to 7 h,
- $\text{pAUC}_{7\text{–}12}$, AUC from 7 to 12 h

Based on these recommendations, the %PE values were assessed using $C_{\max}$, $\text{AUC}_{0\text{-inf}}$, $\text{pAUC}_{0\text{–}3}$, $\text{pAUC}_{3\text{–}7}$, and $\text{pAUC}_{7\text{–}12}$.

Simulation Scenarios

Two simulation scenarios were considered to assess the performance of the time-scaled convolution and deconvolution-based approaches when the IIV on *in vivo* drug release significantly increases (scenario 1) and when complex models were used to characterize the UIR functions (scenario 2).

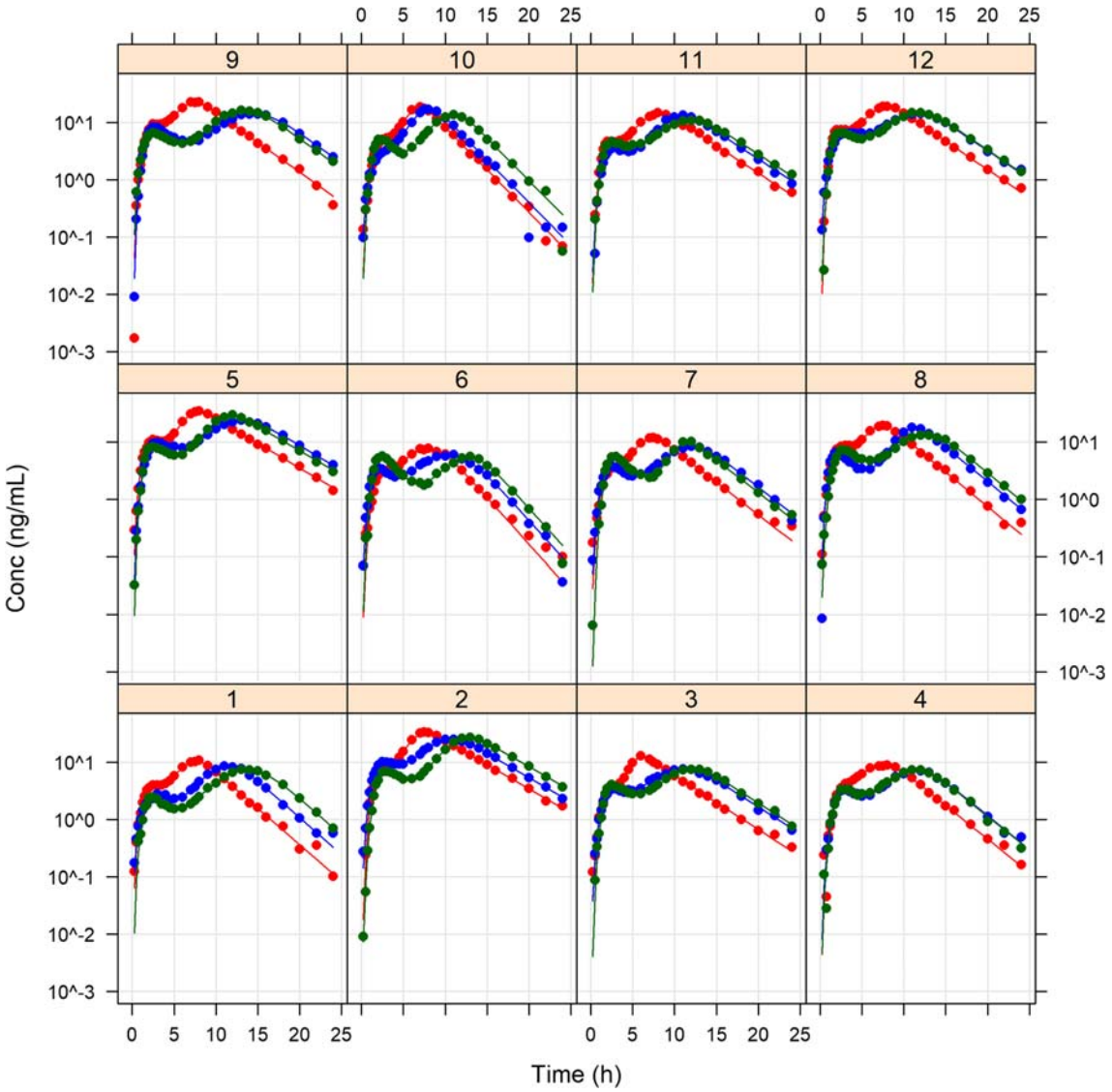

Fig. 3. Method 1–Model 1–Run 2: Observed (dots) and model predicted (solid lines) individual concentrations in the IVIVC analysis for the three formulations. Red, form A; blue, form B; and green, form C

The scenario 1 was evaluated by comparing the performances of model 1 using the convolution and the deconvolution-based approaches when the IIV on *in vivo* drug release ranged from 20 to 50%. The scenario 2 was evaluated by comparing the performances of the convolution and deconvolution-based approaches for model 1 and model 2 at a fixed value of 20% of the IIV on *in vivo* drug release.

Software

All simulations and parameter estimations were conducted using the NONMEM software version 7.4 (ICON Development Solutions, Hanover, MD, USA). The data management and graphical presentation of the results were conducted using the R language (17). The non-compartmental analysis was conducted using the validated and open source R library "NonCompart" (18). The R code used for generating the Levy's plot and the time-scaled dissolution data is provided in the Supplementary file together with the NONMEM code used for the implementing methods 1 and 2.

RESULTS

Step 1—Modeling the Dissolution Data

The double Weibull model (Eq. 5) was independently fitted to the dissolution data of the three formulations. The estimated parameters are presented in Supplementary Table S1 and the plot of the simulated dissolution data with the model predicted values are presented in Fig. 2.

Step 2—Modeling IR Data

The models defining the IR data (Eqs. 7 and 8) were fitted to the data of the 12 subjects using a population approach. The estimated parameters for model 1 and model 2 are presented in Table S2 and Table S3 of the Supplementary material, respectively.

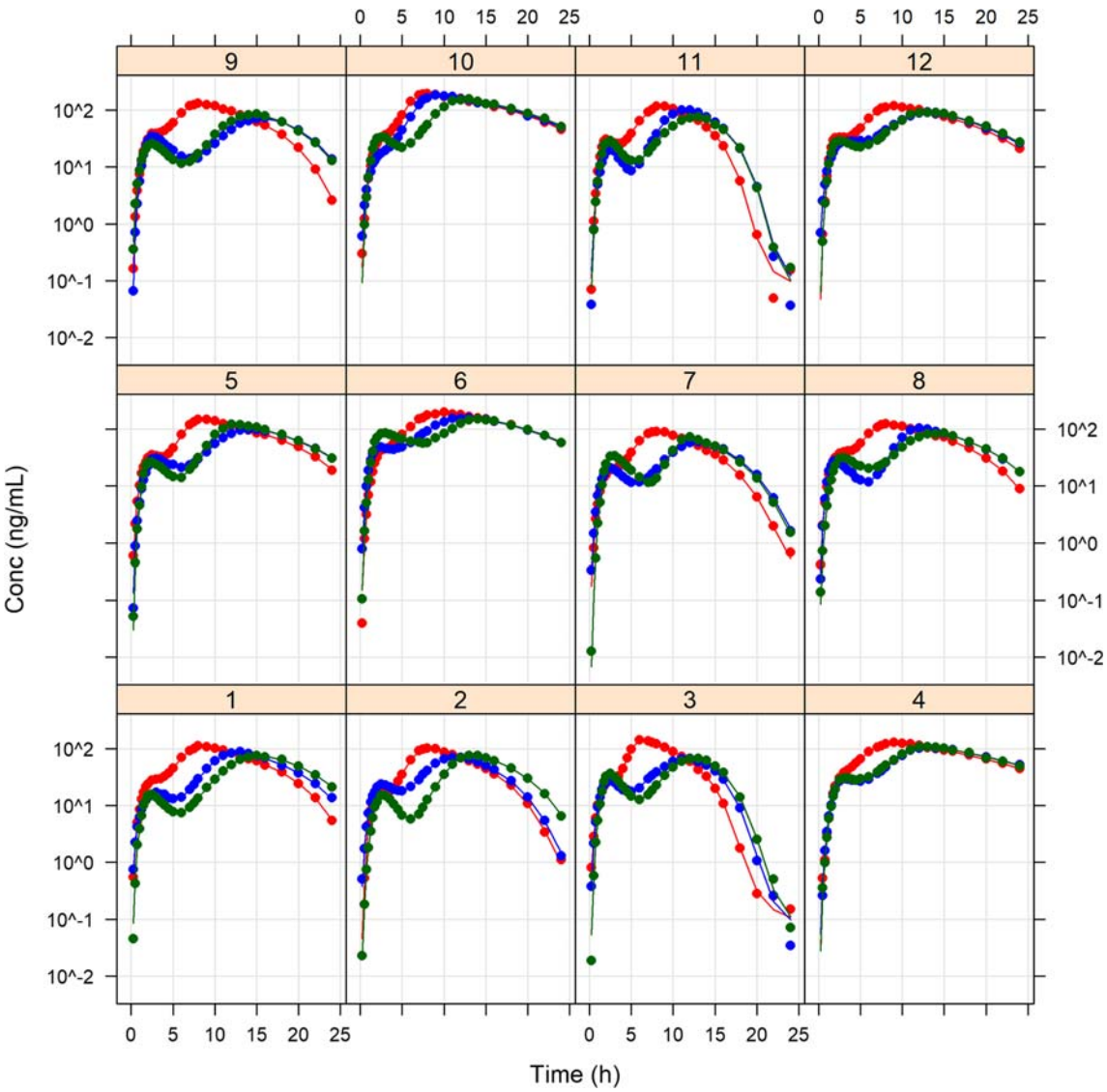

Fig. 4. Method 1–Model 2–Run 2: Observed (dots) and model predicted (solid lines) individual concentrations in the IVIVC analysis for the three formulations. Red, form A; blue, form B; and green, form C

The plots of individual and model predicted plasma concentrations are presented in Supplementary Fig. S2 and S4 for model 1 and model 2, respectively. The adequacy of the model was evaluated by the visual predictive checks (VPC). The individual data of one-hundred subjects were simulated using a Monte Carlo approach using the parameters presented in Tables S2 and S3. The median and 90% prediction intervals from model simulations were plotted along with the data used for estimating the model parameters (Supplementary Fig. S1 and Fig. S3 for model 1 and model 2, respectively). It can be seen from the VPC that the models performed adequately well in describing and predicting the IR data.

The shrinkages of the empirical Bayes parameter estimates were computed to assess whether the parameters (V_i, kel_i for model 1 and V_i, $k12_i$, $k21_i$, Vm_i, and Km_i for model 2) represented reliable estimates of the individual parameters appropriate for the step 2 of the analysis. On overall, the estimated shrinkage values were lower than 20% supporting the use of these parameters in the subsequent analyses. In case of shrinkage values greater than 30%, two options can be considered: (1) the number of subject considered is too small for a correct estimate of the IIV variability, in this case, a study with a larger sample size have to be considered, and (2) a study with larger sample size cannot be conducted, in this case, the IVIVC can be tentatively assessed using the mean and not the individual values.

Step 3—IVIVC Analysis

Method 1. A population analysis on the ER data was initially conducted (run 1) for each simulation scenario assuming no IIV in the parameters of the r(t) function (IIV = 0%) using the convolution-based model (Eqs. 3 and 4) with the individual parameters defining the UIR function fixed to the values estimated in step 2, and the parameters of the r(t) function fixed to the values estimated in the analysis of dissolution data (step 1). The full time-scaling five-parameter model defined in Eq. 9 was included in the initial analysis. The time-scaling parameters were fixed to a common

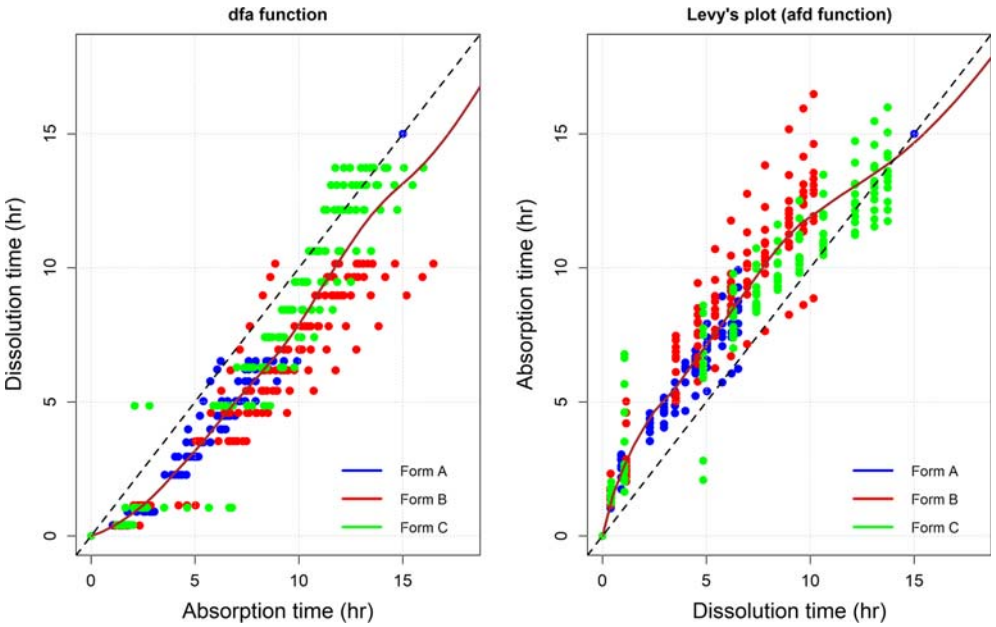

Fig. 5. Model 1—Levy's plot (function adf) and the inverse Levy's plot (function dfa) with the individual data for each formulation (dots). The solid line represents the nonparametric smoothing function and the dotted line represents the reference identity line

value for all formulations and estimated as fixed-effect parameters. No random effect was associated to these parameters to ensure the same time-scaling for all formulations. As an example, the estimated parameters of run 1 for model 1 and 2 are presented in Table I when the simulated IIV on *in vivo* drug release was fixed to 20%. The inspection of the estimated parameters indicated that the parameters a_1, a_2, and b_1 were estimated to 0, 1, and 0 by the nonlinear regression, respectively. Therefore, a second run (run 2) was conducted fixing these parameter values to 0, 1, and 0, and including the IIV effect on *in vivo* drug release as additional parameters. The results of this new analysis are presented in Table I.

The changes in OFV (ΔOFV) were always < 7.81 indicating that the reduced models (run 2) provided a better description of the data ($p < 0.05$, df = 3). Therefore, the time-scaling models defined in run 2 were retained as the final and best performing models.

The plots of the individual observations and model predictions for the three formulations resulting from the analysis conducted in run 2 are presented in Fig. 3 for model 1 and Fig. 4 for model 2. The adequacy of the model was

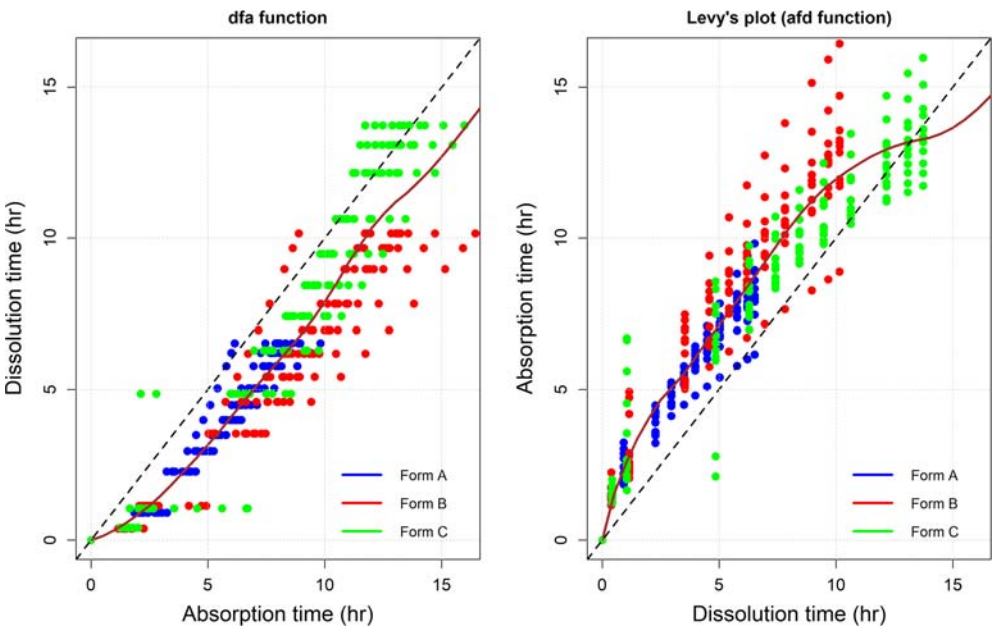

Fig. 6. Model 2—Levy's plot (function adf) and the inverse Levy's plot (function dfa) with the individual data for each formulation (dots). The solid line represents the nonparametric smoothing function and the dotted line represents the reference identity line

evaluated by performing visual predictive checks (VPC). The individual ER data for the three formulations of one-hundred subjects were simulated using a Monte Carlo approach and the parameters presented in Table I. The median and 90% prediction intervals from model (run 2) simulations were plotted along with the data used for estimating the model parameters (Supplementary Fig. S5 and Fig. S6 for model 1 and model 2, respectively). It can be seen from the VPC that the models performed adequately well in describing and predicting the ER data for the three formulations.

Method 2. The deconvolution analysis was conducted for each level of IIV on *in vivo* drug release (20%, 30%, 40%, and 50%) to estimate the individual *in vivo* input function (Eq. 5) using the convolution-based model (Eqs. 3 and 4) with the parameters of the UIR function fixed to the individual IR PK parameters estimated in step 2. The parameters of the Weibull function were estimated by fitting the model to the ER data using a population approach. In the initial run (run 1), the population analysis did not include random effect for the parameters of the Weibull function as IIV was set zero, while the parameters defining the random effect of the Weibull function were included in the analysis of the second run (run 2). The plot of the individual fraction of the dose absorbed *versus* time for method 2 and run 2 is presented in the Supplementary file (Fig. S7 and Fig. S8 for model 1 and model 2, respectively).

The Levy's plot (function afd) and the inverse Levy's plot (function dfa) are presented in Fig. 5 for model 1 and Fig. 6 for model 2. Figures S9 and S10 in the Supplementary file show the dissolution data in the original time frame, the time-scaled dissolution data, and the individual data resulting from the deconvolution analysis for each formulation and for model 1 and model 2.

Step 4—Model Validation

According the FDA guidelines, the validation criteria of an IVIVC analysis should satisfy the two conditions for each PK parameter considered: the average absolute percent prediction error (% PE) should be of 10% or less, and the maximal %PE value for each formulation should not exceed 15%.

Due to the large number of simulations considered in the analysis, the results were visualized using radar charts showing the average and maximal %PE values for each PK parameter and simulation scenario. On these charts, each spoke represents the performances of each PK parameter (C_{max}, AUC_{inf}, AUC_{0-3}, AUC_{3-7}, and AUC_{7-12}).

Figure 7 shows the comparison of the performances of the convolution and deconvolution-based approaches for model 1 and model 2 at a fixed IIV value of 20% on *in vivo* drug release. Panels (**a**) and (**b**) show the %PE average values and the maximal %PE values for the deconvolution-based approach for models 1 and 2, respectively. Panels (**c**) and (**d**) show the %PE average values and the maximal %PE values for the convolution-based approach for models 1 and 2, respectively. The results indicate that the performances of the convolution-based approach remain constant and within the acceptability criteria for internal validation for the two models. However, the performance of the deconvolution-

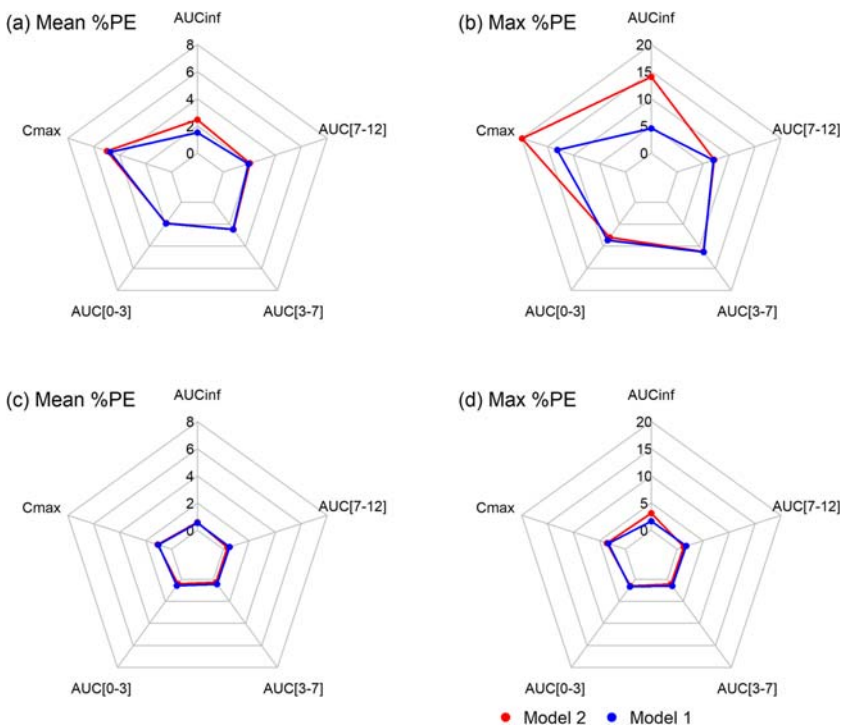

Fig. 7. Comparison of the performances of the convolution and deconvolution-based approaches for model 1 and model 2 at a fixed IIV value of 20% on *in vivo* drug release. Panels **a** and **b** show the %PE average values and the maximal %PE values for the deconvolution-based approach for model 1 and 2, respectively. Panels **c** and **d** show the %PE average values and the maximal %PE values for the convolution-based approach for model 1 and 2

based approach seems significantly affected by the complexity of the UIR model: the maximum %PE for C_{max} exceeds the acceptability criteria, while the average %PE remains in the acceptable ranges (< 6%) for each PK parameter.

Figure 8 shows the comparison of the performances of the convolution and the deconvolution-based approaches for model 1 for increasing values of IIV on *in vivo* drug release from 20 to 50%. Panels (**a**) and (**b**) show the %PE average values and the maximal %PE values for the deconvolution-based approach. Panels (**c**) and (**d**) show the %PE average values and the maximal %PE values for the convolution-based approach. The results indicate that the performances of the convolution-based approach remain constant and within the acceptability criteria for internal validation for IIV on *in vivo* drug release ranging from 20 to 50%. However, the performance of the deconvolution-based approach seems significantly affected by the level of IIV: the maximum %PE for C_{max} exceeds the acceptability criteria, while the average %PE remains in the acceptable ranges (< 6%) for each PK parameter.

DISCUSSION

The simulation study provided a quantitative framework for illustrating how IVIVC can be implemented using alternative analysis methods and for comparing the performances of alternative approaches for dealing with different time frames of dissolution and *in vivo* absorption processes.

Two methodologies have been presented. The convolution-based approach (method 1) presents the advantage to implement the IVIVC with an assessment of the time-scaling between *in vitro* and *in vivo* processes in one single analysis step using a nonlinear mixed-effect modeling approach. The quality and the predictive performances of the model can be evaluated by comparing the observed with the model predicted *in vivo* concentrations using the standard tools for model validation as reported in the FDA guidance for population modeling (19). The presence or the absence of a time-scaling can be formally assessed using the standard statistical tools by comparing the performances of models with and without time-scaling. The limitation of this approach is that a formal model describing the time-scaling is requested; however, this limitation is someway mitigated by the possibility of comparing alternative models using standard statistical tools.

The deconvolution-based approach (method 2) requires few additional analysis steps but presents the advantage to graphically visualize the presence of a time-scaling between *in vitro* and *in vivo* processes and to time scale the dissolution data using a nonparametric approach. No formal model is requested to assess the time-scaling as this is numerically estimated using a nonparametric smoothing function used to fit the Levy's and the inverse Levy's plots.

One of the nice features of the methodology presented in this paper is that the same convolution integral model implemented using a set of differential equations can be used to evaluate a time-scaled IVIVC using either the deconvolution or the convolution-based approach.

The traditional approaches for conducting a deconvolution are based on specific and sophisticated numer-

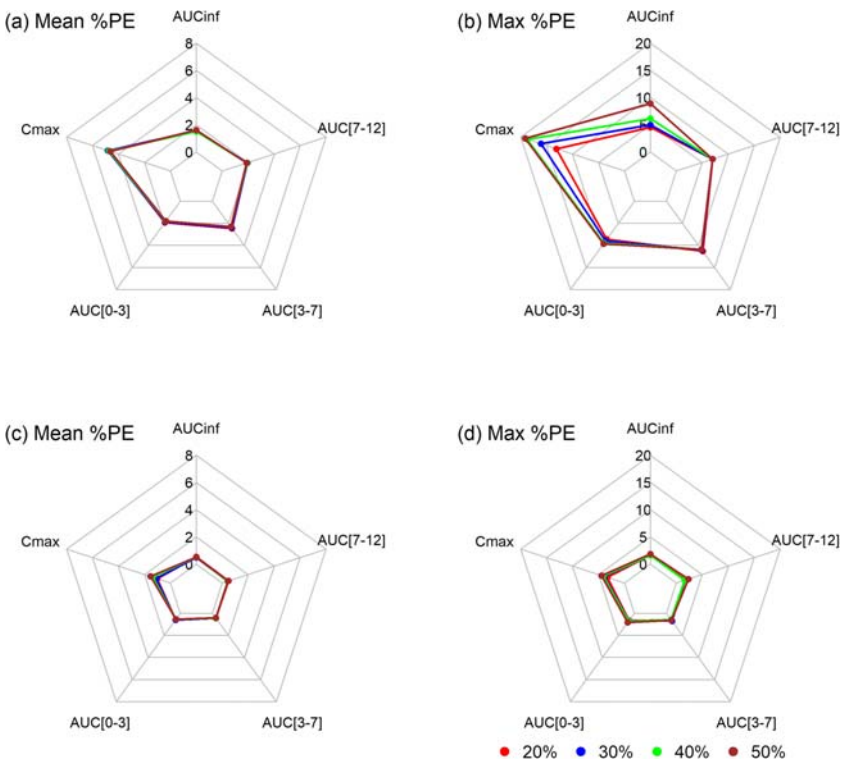

Fig. 8. Comparison of the performances of the convolution and the deconvolution-based approaches for model 1 for increasing values of IIV on *in vivo* drug from 20 to 50%. Panels **a** and **b** show the %PE average values and the maximal %PE values for the deconvolution-based approach. Panels **c** and **d** show the %PE average values and the maximal %PE values

ical algorithms such as Fourier transforms, system identification, constrained optimization, cubic spline functions, maximum entropy, and genetic algorithm (20). All these methods require sometime unrealistic constraints to allow the stable implementation of the selected algorithms that have to be implemented using specific software tools. At variance of these methods, the deconvolution analysis method proposed in this paper can be easily implemented using the same nonlinear mixed-effect approach and standard modeling software (such as NONMEM) used for the convolution-based approach without the need of implementing sophisticated numerical deconvolution algorithms in dedicated software.

The example presented was based on a dissolution/absorption described by a model represented by a Weibull function. However, this method has been shown to account for any parametric and nonparametric functions (10).

Traditionally, the IVIVC analysis is conducted on the average *in vitro* and *in vivo* data. In the present analysis, IVIVC was conducted using the individual data and a population approach. This approach has been shown to present a number of advantages with respect to method based on the averaging of data. In particular, the comparison of the population *versus* the data averaging indicated that averaging has a significant impact on the accuracy of predictions (21,22).

In addition, another important difference in the average *versus* population approach is that the population approach allows for evaluating the potential impact of IIV in the absorption process on the predicted bioavailability.

The objective of the IVIVC analysis was to estimate the magnitude of the error in predicting the *in vivo* bioavailability results from *in vitro* dissolution data. This is the reason why it was critical to evaluate and consider in the analysis all factors that could affect the predictions and the uncertainty on the predictions. The average %PE values estimated with the two methods in the different simulation scenarios were below the critical value of 10%. However, the maximal values of %PE estimated with the deconvolution-based approach were significantly affected either by the increase of the IIV on *in vivo* drug release or by the complexity of the UIR model leading to results failing to comply with the IVIVC validation criteria (maximal %PE >15%). The convolution-based modeling approach provided more robust and stable results in the different simulation scenarios with statistically better performances associated with the inclusion of random effect on the *in vivo* drug release parameters. An additional reason for considering the convolution-based modeling approach as the reference method has been illustrated in a recent paper where this method has been applied in a general in silico modeling and simulation framework for identifying optimal doses and *in vitro*/*in vivo* release properties providing an optimized benefit-risk ratio of a treatment (1). In addition to the findings of this previously published paper, the present analysis provides quantitative criteria for (i) comparing the performances of different methodologies for the assessment of time-scaled IVIVC, and (ii) quantifying the impact of complex UIR models and large IIV on *in vivo* drug release on the performance of IVIVC in a population-based modeling framework.

CONCLUSION

Different analyses were conducted to assess the impact of complex UIR models (one-compartment linear *versus* two-compartment with nonlinear elimination) and the impact of increasing levels of IIV (20%, 30%, 40%, and 50%) on *in vivo* drug release. The results indicated that the deconvolution-based method is much more sensitive than the convolution-based method to the complexity of the UIR model as well as to the level of IIV leading to results that fail to support IVIVC. At variance of these results, the performance of the convolution-based approach seems independent of the complexity of the UIR model as well as of the level of IIV. These findings indicated that the convolution-based approach should be considered the preferred approach for assessing IVIVC.

REFERENCES

1. Gomeni R, Fang LL, Bressolle-Gomeni F, Spencer TJ, Faraone SV, Babiskin A. A general framework for assessing *in-vitro*/in-vivo correlation as a tool for maximizing the benefit-risk ratio of a treatment using a convolution-based modeling approach. CPT Pharmacometrics Syst Pharmacol. 2019;8(2):97–106.
2. Wagner JG, Nelson E. Kinetic analysis of blood levels and urinary excretion in the absorptive phase after single doses of drug. J Pharm Sci. 1964;53:1392–403.
3. Loo JCK, Riegelman S. New method for calculating the intrinsic absorption rate of drugs. J Pharm Sci. 1968;57(6):918–28.
4. Cutler DJ. Numerical deconvolution by least squares: use of prescribed input functions. J Pharmacokinet Biopharm. 1978;6(3):227–41.
5. Pitsiu M, Sathyan G, Gupta S, Verotta D. A semiparametric deconvolution model to establish in-vivo-in-vitro correlation applied to OROS oxybutynin. J Pharm Sci. 2001;90(6):702–12.
6. Gaynor C, Dunne A, Davis J. A comparison of the prediction accuracy of two IVIVC modelling techniques. J Pharm Sci. 2008;97(8):3422–32.
7. Buchwald P. Direct differential-equation-based in-vitro-in-vivo correlation (IVIVC) method. J Pharm Pharmacol. 2003;55(4):495–504.
8. Gaynor C, Dunne A, Costello C, Davis J. A population approach to *in-vitro*-in-vivo correlation modelling for compounds with nonlinear kinetics. J Pharmacokinet Pharmacodyn. 2011;38(3):317–32.
9. Hovorka R, Chappell MJ, Godfrey KR, Madden FN, Rouse MK, Soons PA. CODE: a deconvolution program implementing a regularization method of deconvolution constrained to non-negative values. Description and pilot evaluation. Biopharm Drug Dispos. 1998;19:39–53.
10. Gomeni R, Bressolle-Gomeni F. Deconvolution analysis by non-linear regression using a convolution-based model: comparison of nonparametric and parametric approaches. AAPS J. 2019;22(1):9.
11. U.S. Department of Health and Human Services, Food and Drug Administration (1997) Guidance for industry: extended release oral dosage forms: development, evaluation, and application of *in-vitro*/in-vivo correlations 1997. https://www.fda.gov/media/70939/download. Accessed Feb 3 2020.
12. Rescigno A. Compartmental analysis and its manifold applications to pharmacokinetics. AAPS J. 2010;12(1):61–72.
13. Mould DR, Upton RN. Basic concepts in population modeling, simulation, and model-based drug development—part 2: introduction to pharmacokinetic modeling methods. CPT Pharmacometrics Syst Pharmacol. 2013;2:e38.

14. Brent RP. Algorithms for minimization without derivatives. Englewood Cliffs: Prentice-Hall; 1973.
15. Cleveland WS. Robust locally weighted regression and smoothing scatterplots. J Am Stat Assoc. 1979;74(368):829–36.
16. U.S. Department of Health and Human Services, Food and Drug Administration, Center for Drug Evaluation and Research (CDER). Draft guidance on methylphenidate hydrochloride. https://www.accessdata.fda.gov/drugsatfda_docs/psg/Methylphenidate%20Hydrochloride_draft_Oral%20tab%20ER_RLD%2021121_RC07-18.pdf. 2018. Accessed Feb 3 2020.
17. The R Project for Statistical Computing. R. http://www.r-project.org/ Accessed Feb 3 2020.
18. Kim H, Han S, Cho YS, Yoon SY, Bae KS. Development of R packages: 'NonCompart' and 'ncar' for noncompartmental analysis (NCA). Transl Clin Pharmacol. 2018;26(1):10–5.
19. U.S. Department of Health and Human Services, Food and Drug Administration, Center for Drug Evaluation and Research (CDER). Population pharmacokinetics guidance for industry DRAFT GUIDANCE July 2019 https://www.fda.gov/media/128793/download. Accessed Feb 3 2020.
20. Madden FN, Godfrey KR, Chappell MJ, Hovorka R, Bates RA. A comparison of six deconvolution techniques. J Pharmacokinet Biopharm. 1996;24:283–99.
21. Gaynor C, Dunne A, Davis J. The effects of averaging on accuracy of IVIVC model predictions. J Pharm Sci. 2009;98(10):3829–38.
22. Ostrowski M, Wilkowska E, Baczek T. The influence of averaging procedure on the accuracy of IVIVC predictions: immediate release dosage form case study. J Pharm Sci. 2010;99(12):5040–5.